Computational and Theoretical Chemistry 1009 (2013) 1–7

Contents lists available at SciVerse ScienceDirect

Computational and Theoretical Chemistry

journal homepage: www.elsevier.com/locate/comptc

High reactivity of nitric oxide with peroxo groups on BaO particles. DFT calculations

Carolina Zubieta [a,*], Norberto J. Castellani [a], Ricardo M. Ferullo [b]

[a] IFISUR, Universidad Nacional del Sur, Av. Alem 1253, CP 8000 Bahía Blanca, Argentina
[b] INQUISUR, Universidad Nacional del Sur, Av. Alem 1253, CP 8000 Bahía Blanca, Argentina

ARTICLE INFO

Article history:
Received 20 September 2012
Received in revised form 17 December 2012
Accepted 20 December 2012
Available online 5 January 2013

Keywords:
NO
BaO particle
Peroxo
NO_x storage
DFT

ABSTRACT

The reactivity of NO with peroxo groups (O_2^{2-}) present on Ba_6O_6 particles is studied using the density functional theory (DFT). Bulk-like and hexagonal structures were considered. The surface peroxo groups were modeled by adding an oxygen atom (O_a) to a structural oxygen anion (O_s). Calculations indicate that the NO molecule can react either with O_s or, with O_a to form NO_2 by surpassing an activation barrier of only 0.2 eV or less. In particular, the NO_2 formation via the extraction of O_s involves a transition state in which an interchange is produced between O_a and O_s. The predicted high reactivity is in agreement with experiments performed on highly defective samples of BaO wherein NO activation is observed to occur on surface peroxo groups.

1. Introduction

The removal of harmful exhaust gases poses a great challenge to the development of novel catalytic materials such as the so called NO_x Storage and Reduction catalysts (NSR catalysts). In these systems, nitrogen oxides are stored during long oxygen excess periods and reduced to N_2 during short fuel rich periods. Usually, dispersed BaO is used as a storage material which is able to trap NO_x as surface nitrites and nitrates. For this reason, in the last years the storage of NO_x has been extensively studied on supported BaO catalysts [1–10] as well as on films [11–13] and powders [14] of this oxide. On the other hand, many fundamental aspects on NO_x interaction with BaO could be understood by means of density functional calculations [15–23].

Dissociative adsorption of O_2 on surfaces of alkaline-earth oxides occurs through the formation of peroxo groups, O_2^{2-} (also called peroxide groups). Adding an O atom to the stoichiometric surface of an alkaline-earth oxide implies that two O atoms have the general oxidation state of −2, and hence are bound as an O_2^{2-} ion. The process of peroxo formation has been investigated theoretically by several authors. Kantorovich and Gillan have studied peroxo groups formed at terrace and low-coordinated sites of MgO [24]. This subject was reconsidered by Geneste et al. [25]. Peroxo groups formed at the (1 0 0) surface of CaO and BaO were investigated by Strömberg and Lu et al., respectively [26,27]. Systematic studies of peroxo groups formed on alkaline-earth oxides have been reported by Karlsen et al. [28], Abdel Halim and Shalabi [29], and Di Valentin et al. [30].

On the other hand, the reactivity of peroxo on BaO was intensively analyzed by Lunsford et al. [1–4]. They studied the NO_2 storage over BaO supported on MgO with the *in situ* Raman spectroscopy and found that the preoxidation of the catalyst or exposure to oxygen leads to the formation of peroxo groups that enhance the rate for nitrate formation [1]. By studying the catalytic decomposition of NO on BaO/MgO, they also noticed that the NO activation occurs on O_2^{2-} ions that are present on defect-rich BaO [2,4].

Although the structure of BaO operating as a storage material is not clear, it is expected to present very different topological defects which can be easily modeled with very small particles. In fact, it is well known that nanoscale alkaline-earth metal oxides are very active for a large number of reactions including chemical synthesis and pollution control [31,32]. They exhibit unusual surface morphologies and possess a large number of reactive sites due to the presence of high concentrations of defects such as edges and corners. In the past, DFT calculations performed with small particles of alkaline-earth oxides were used as a complementary tool to investigate the adsorption properties and reactivity of dispersed or polycrystalline oxides [14,33–35].

The main interest of this research was to evaluate the role played by peroxo groups on Ba_6O_6 particles during its interaction with NO by means of the density functional theory (DFT). This process has an important environmental and technological significance, and up to now, it has not been studied at a fundamental level. We have attempted here to provide a rationale for the high capacity for NO storage of highly defective BaO. On the other hand, admitting that the Ba_6O_6 particles used in the present calculations should not be considered as models of Ba(1 0 0) surfaces but as iso-

* Corresponding author. Tel.: +54 291 4595141; fax: +54 291 4595142.
E-mail address: czubieta@uns.edu.ar (C. Zubieta).

2210-271X/$ - see front matter © 2013 Elsevier B.V. All rights reserved.
http://dx.doi.org/10.1016/j.comptc.2012.12.026

lated particles, the use of these tiny systems can be used as a guide in the study of different aspects of adsorption. Additionally, in simulations of chemical reactions it is essential to have a reliable methodology for searching transition states, and very often, they are formed by complex molecular structures that are more easily tractable with small systems.

2. Computational details

Density functional theory (DFT) calculations were carried out by using the gradient-corrected Becke's three parameters hybrid exchange functional, in combination with the correlation functional of Lee, Yang and Parr (B3LYP) [36]. This method was widely used in the past to study adsorption processes yielding reliable results both on oxides and metal clusters. All the calculations have been performed using the Gaussian-03 program package [37].

The interaction between NO and BaO was evaluated by using two different structures of the Ba_6O_6 particle: one conserving the bulk structure, denoted here as the "slab" structure, and the other considering a hexagonal geometry (Fig. 1). As in Ref. [38], we observed that both structures are essentially isoenergetic (the slab structure is only 0.1 eV more stable). These models will be denoted as "Ba_6O_6(slab)" and "Ba_6O_6(hex)", respectively. On the Ba_6O_6(slab) particle two non-equivalent peroxo groups can be formed by adsorbing an O atom to structural O anions located on edge and corner sites. In Ba_6O_6(hex) all the structural oxygen anions are equivalent. The systems with peroxo groups are indicated as "O–Ba_6O_6". In both geometries, the NO molecule can interact either with the structural oxygen of the peroxo group (O_s), or with the external (or adsorbed) oxygen (O_a). N and O atoms have been described at the all-electron level using the 6-31+G* basis set. The Ba atoms have been treated with the LANL2DZ basis set [39]. The adsorption energy E_{ads} was evaluated according to the following total energies difference:

$$E_{ads} = E(\mathrm{NO/O{-}Ba_6O_6}) - E(\mathrm{O{-}Ba_6O_6}) - E(\mathrm{NO})$$

According to this definition, negative values correspond with exothermic processes. The energy difference calculated in this way present an error known as basis set superposition error (BSSE). When two fragments interact each fragment takes the basis functions of the other, and as a consequence, the energy of the system falls down and the magnitude of the energy difference is overestimated. To correct this error we applied the so-called counterpoise (CP) procedure [40,41] in which each fragment is treated with the ghost functions of the other one. Activation energies were determined for the transition between chemisorbed NO species and NO_2 formation via the interaction with peroxo. In the calculation of the potential energy curve, the sum of O–Ba_6O_6 and NO total energies was used as reference. This energy difference was simply labeled as "ΔE". Thus, ΔE coincides with E_{ads} at the optimized structures for the interaction of NO with O–Ba_6O_6. Besides, ΔE values at transition states and at the final products were also corrected by CP. In all cases, the correction was performed *a posteriori*, i.e., by a single point calculation on the structures optimized by the standard procedure. The magnitude of the BSSE resulted to be around 0.2 eV. We also observed that the values of ΔE were slightly affected with the CP correction.

Vibrational frequencies have been computed by determining the second derivate of the total energy with respect to the internal coordinates. The atomic net charges were calculated following the NBO (Natural Bond Orbital) analysis [42]. The location of transition states was performed using the Synchronous Transit-Guided Quasi-Newton Method (STQN) [43] implemented in Gaussian 03.

3. Results and discussion

3.1. Surface peroxo complexes

Firstly, we analyze the structure of surface peroxo groups formed on Ba_6O_6(hex) and on edge and corner sites of Ba_6O_6(slab). The main results are presented in Table 1 and Fig. 2. In all cases the O_s–O_a bond length is about 1.51 Å. Very similar values were found for O adsorption on the BaO(100) surface, and on edge and corner defects using B3LYP and the embedding cluster approach [27,30]. In these three situations the O_a atom is electrostatically linked with two Ba cations, as it can be deduced looking at the calculated NBO charges. The O_a–Ba distance has a value of about 2.70 Å at corner site of Ba_6O_6(slab) and Ba_6O_6(hex), and 2.84 Å at edge on Ba_6O_6(slab).

We have also computed the vibrational frequencies for the stretching mode of the peroxo groups (Table 1). The corresponding values, around 860 cm^{-1}, are consistent with different experimental measurements reported in the literature. For instance, Nakamura et al. assigned a value of 880 cm^{-1} to peroxo groups formed by decomposition of N_2O on the surface of CaO [44]. Hess and Lunsford assigned features within the range of 900–980 cm^{-1} to surface peroxo groups present on defect-rich BaO, whereas a band at 830 cm^{-1} was observed in crystalline BaO_2 [1]. Di Valentin et al. calculated a value of 907 cm^{-1} on the Ba(100) surface by using DFT [30]. As shown in Table 1, in all cases the peroxo charge is $-1.96e$, with O_s slightly more charged than O_a. Similar results were found by Lu et al. [27] on terrace and topological defects of BaO.

3.2. NO adsorption on Ba_6O_6 in absence of peroxo groups

NO adsorption on Ba_6O_6 in absence of peroxo groups is shown in Fig. 3. Some selected results are reported in Table 2. The N–O distance stretches from 1.157 Å at gas phase to 1.31–1.35 Å when it is adsorbed on the BaO particles. The O_s–N–O angle is around 110°. On the other hand, the oxygen atom of NO is electrostatically linked with a Ba cation. The O–Ba distance is about 2.75 Å for Ba_6O_6(hex) and on corner site of Ba_6O_6(slab), and it is somewhat longer at edge of the cubic-type cluster (2.82 Å).

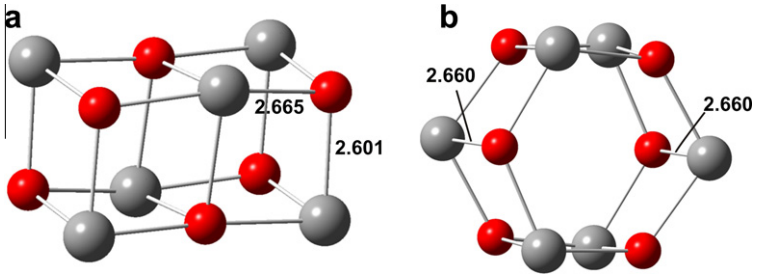

Fig. 1. Optimized structures of the oxides particles: (a) Ba_6O_6(slab) and (b) Ba_6O_6(hex).

Table 1
Peroxo groups on the Ba_6O_6 particles. Charges (q) and stretching vibration mode (ν). O_s is the surface oxygen atom and O_a is the external oxygen atom.

	Ba_6O_6(slab) edge	Ba_6O_6(slab) corner	Ba_6O_6(hex)
$q(O_s)$	−1.03	−1.05	−1.05
$q(O_a)$	−0.93	−0.91	−0.91
$q(O_sO_a)$	−1.96	−1.96	−1.96
$\nu(O_s–O_a)$ (cm^{-1})	864	858	850

Table 2
NO adsorbed on the Ba_6O_6 particles in absence of peroxo groups. Adsorption energies (E_{ads}), charges (q), and stretching (ν) and bending (δ) vibrational modes.

	Ba_6O_6 (slab) edge	Ba_6O_6 (slab) corner	Ba_6O_6 (hex)
E_{ads} (eV)	−1.60	−1.57	−1.70
q(N)	−0.11	−0.09	−0.14
q(O)	−0.79	−0.72	−0.85
q(NO)	−0.90	−0.81	−0.99
$q(O_s)$	−1.01	−1.08	−0.91
ν(N–O) (cm^{-1})	1187	1221	1114
$\nu(O_s–N)$	850	790	920
$\delta(O_s–N–O)$	656	638	650

NO is bonded with E_{ads} values of about −1.6 eV for both bulk-type particles, while on the hexagonal structure it is 0.1 eV more stable. Interestingly, these values are very similar than the one calculated for NO adsorption on the BaO(100) surface by using periodic DFT (about −1.5 eV) [20,22]. This similarity on the adsorption strength between particles and surfaces was also noted in a related system. Indeed, a weak dependence on cluster size was observed by Grönbeck et al. [15] during the NO_2 adsorption on different BaO particles, with a rapid convergence as the particle size increases. In particular, the NO_2 adsorption is only 0.2 eV stronger on the extended BaO(100) surface than on the Ba_6O_6 bulk-like particle.

The NO net charge is negative, from about −0.8 to −1*e*, indicating an electron charge transfer from the BaO surface to the adsorbate. From Table 2 is clear that this charge is mainly taken from O_s. Indeed, the magnitude of the negative charge of O_s decreases by about 0.8*e* in comparison with the bare particle. The NO electronic charge is localized on the O atom, while the nitrogen atom is almost neutral. Therefore, when NO reacts with BaO surface, it forms a nitrite-like structure if the surface oxygen anion is considered in the molecular structure. Using X-ray photoelectron spectroscopy Schmitz and Baird proposed the same type of molecular adsorption when NO interacts with polycrystalline BaO [13].

The elongation of the NO bond causes a consequent decrease in the N–O stretching frequency. The N–O stretching for free NO is 1978 cm^{-1}. Upon NO adsorption the N–O stretching shifts to 1221 cm^{-1}, 1187 cm^{-1} and 1114 cm^{-1} for corner and edge of Ba_6O_6(slab), and on Ba_6O_6(hex), respectively. Besides, stretching modes in the range of 790–920 cm^{-1} were obtained for the O_s–N bond. For comparison, Xie et al. using Raman spectroscopy assigned features at 1336 and 807 cm^{-1} to adsorbed complexes in which the NO_2 fragment would be linked to a Ba cation via one oxygen atom [4].

3.3. NO reaction with peroxo groups on Ba_6O_6 particles

The main adsorption properties for the non-dissociative NO interaction with peroxo groups on Ba_6O_6 particles are reported in Table 3. NO adsorbs on both oxygen atoms of peroxo with adsorption energies in the range of −0.5/−0.8 eV, i.e., appreciably weaker than on pure Ba_6O_6. The strength of the adsorption follows the order: BaO(hex) > BaO(slab), corner > BaO(slab), edge. In Fig. 4a and a′, Fig. 5a and a′, Fig. 6a and a′ the optimized geometries are schematized. In agreement with the E_{ads} values, the distance between O_s (or O_a) and N is longer than that in absence of peroxo, between 1.7 and 2.3 Å, being longer when the interaction occurs on O_s. On the other hand, the N–O distance stretches to values within the range of 1.19–1.23 Å, and the N–O stretching frequencies decrease to values between 1489 and 1745 cm^{-1} for the different sites and geometries (Table 3). Also here, but less pronounced, a charge

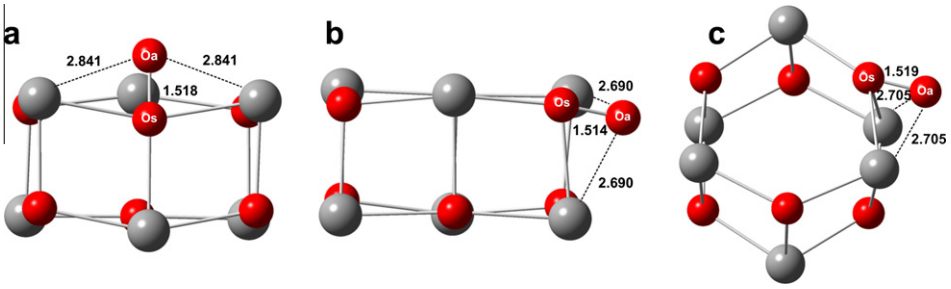

Fig. 2. Structure of a peroxo group on the Ba_6O_6 particles: (a) at the edge site of the Ba_6O_6(slab) particle; (b) at the corner site of the Ba_6O_6(slab) particle; (c) on the Ba_6O_6(hex) particle.

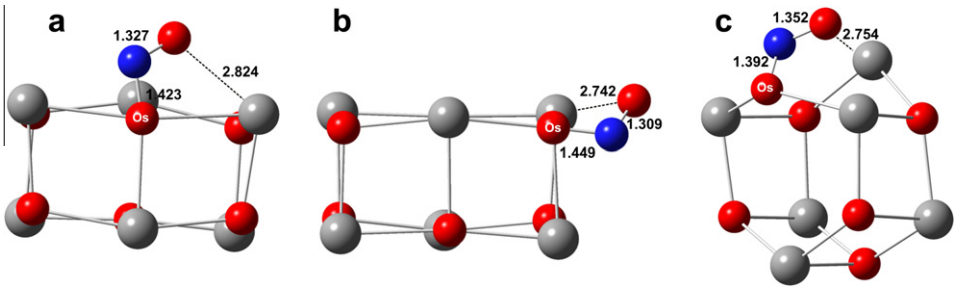

Fig. 3. Adsorption geometries of NO adsorbed on: (a) at the edge site of the Ba_6O_6(slab) particle; (b) at the corner site of the Ba_6O_6(slab) particle; (c) on the Ba_6O_6(hex) particle.

Table 3
NO adsorbed on peroxo groups on the Ba_6O_6 particles. Adsorption energies (E_{ads}), charges (q), and stretching (ν) and bending (δ) vibrational modes. O_s is surface oxygen atom and O_a is the external oxygen atom.

	Ba_6O_6 (slab) edge		Ba_6O_6 (slab) corner		Ba_6O_6 (hex)	
	O_a	O_s	O_a	O_s	O_a	O_s
E_{ads} (eV)	−0.54	−0.51	−0.64	−0.66	−0.81	−0.69
q(N)	0.06	−0.03	0.01	−0.05	0.02	−0.08
q(O)	−0.46	−0.37	−0.57	−0.38	−0.52	−0.30
q(NO)	−0.40	−0.40	−0.56	−0.43	−0.50	−0.38
$q(O_a)$	−0.64	−0.81	−0.46	−0.77	−0.57	−0.77
$q(O_s)$	−0.92	−0.76	−0.93	−0.76	−0.89	−0.81
$q(O_aO_s)$	−1.56	−1.57	−1.39	−1.53	−1.46	−1.58
ν(N–O) (cm^{-1})	1605	1675	1489	1679	1547	1745
$\nu(O_a–O_s)$	902	903	926	917	917	903
$\delta(ONO_a)$ or $\delta(ONO_s)$	517	464	622	481	579	438

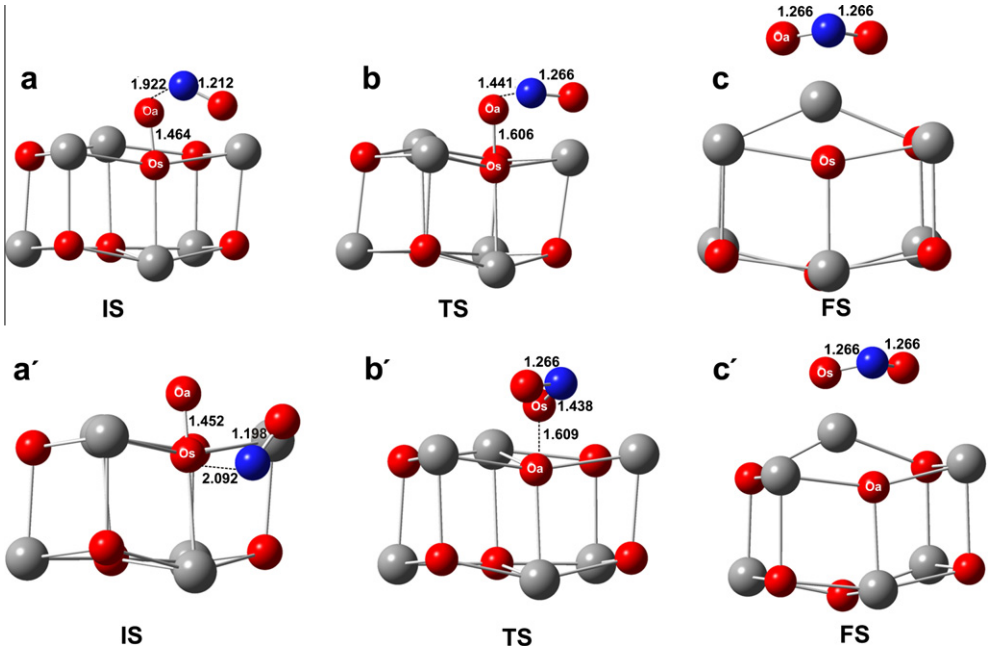

Fig. 4. Optimized structures of NO reaction with the O_a atom of the peroxo group at the edge site of the Ba_6O_6(slab) particle. (a) initially adsorbed structure (the initial state, IS); (b) transition state (TS); (c) the reaction product: adsorbed NO_2 (the final state, FS). (a′), (b′) and (c′) correspond to the same states but with the O_s atom of the peroxo group.

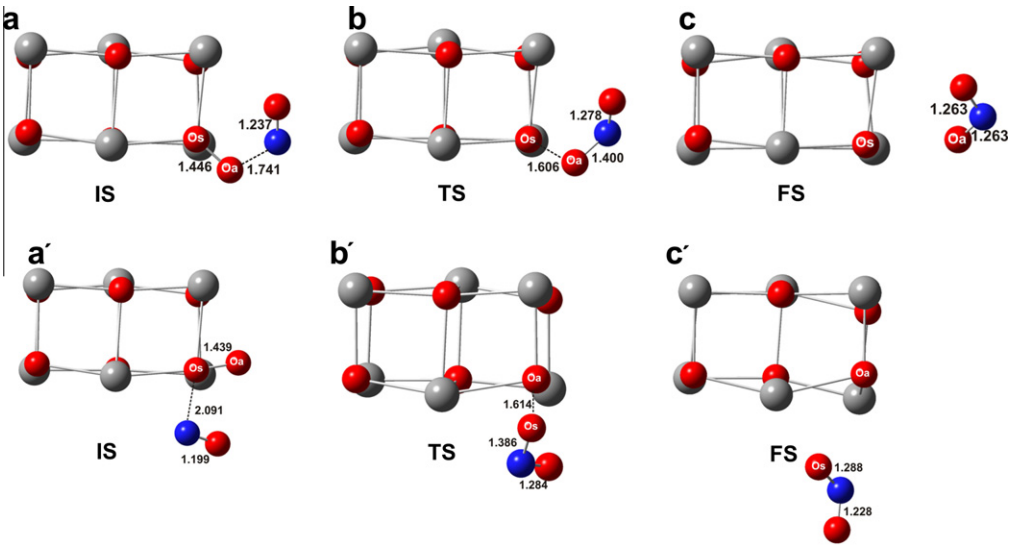

Fig. 5. As in Fig. 4 for the optimized structures of NO reaction with the peroxo group at the corner site of the Ba_6O_6(slab) particle.

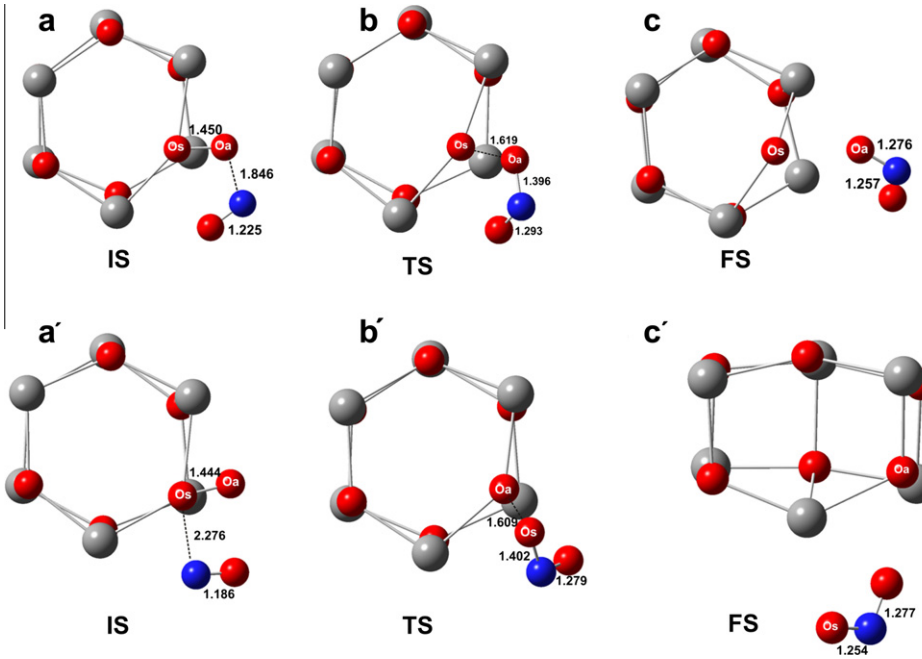

Fig. 6. As in Fig. 4 for the optimized structures of NO reaction with the peroxo group on the Ba_6O_6(hex) particle.

Table 4
Activation energy (E_{act}) and energetic difference (ΔE_{react}) between the final state (adsorbed NO_2) and the initial state (adsorbed NO).

	Ba_6O_6(slab) edge		Ba_6O_6(slab) corner		BaO(hex)	
	O_a	O_s	O_a	O_s	O_a	O_s
E_{act} (eV)	0.19	0.19	0.15	0.04	0.19	0.13
ΔE_{react} (eV)	−2.01	−2.01	−1.85	−1.98	−1.91	−2.38

transfer occurs to NO. The negative charge that NO acquires is taken from the peroxo groups which loses part of its charge (see Tables 1 and 3).

Next, for each case of NO adsorption above considered we proceed to study the reaction towards NO_2. In Figs. 4–6, the optimized molecular structures for the initial state (IS, adsorbed NO), transition state (TS) and final state (FS, adsorbed NO_2) are represented. When NO adsorbs on O_a for both positions, edge and corner, it is extracted to form NO_2. In contrast, when NO interacts with O_s, an atomic interchange is produced; namely, whereas O_a becomes part of the BaO particle structure, the initially structural oxygen (O_s) is released to react with NO and to form NO_2.

In Table 4, the energetic differences (ΔE_{react}) between FS and IS are presented. Clearly, for all cases the reaction is exothermic, with ΔE_{react} values between −1.85 and −2.38 eV. We have also determined the activation barriers to nitrite formation, E_{act}, as it is shown in Table 4. The E_{act} are very low in all cases, about 0.2 eV at the most, indicating a notable reactivity of the peroxo groups. Considering in particular the reaction which implies the extraction of O_a, the corner site of Ba_6O_6(slab) presents a slightly shorter barrier (0.15 eV) with respect to the other two cases. Regarding the reaction with O_s, also here the same site presents the lowest E_{act} value of only 0.04 eV. A schematic potential energy curve for the NO reaction with the O_a atom of the peroxo group at the corner site of the Ba_6O_6(slab) particle is presented in Fig. 7. The profiles for the other cases (not shown) are very similar (see Table 4).

In relation to the final state, complementary calculations on gas phase NO_2 show the following vibrational modes: 1621 cm^{-1} (ν_{asym}), 1320 cm^{-1} (ν_{sym}) and 648 cm^{-1} (δ). When NO_2 is adsorbed the stretching modes decrease and the bending ones increase (see

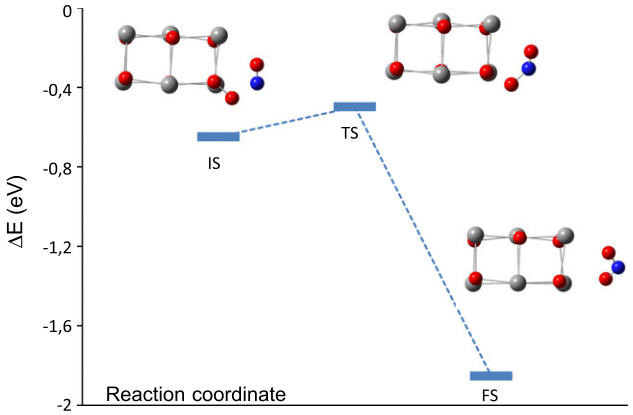

Fig. 7. Schematic potential energy curve for NO reaction with the O_a atom of the peroxo group at the corner site of the Ba_6O_6(slab) particle. The profiles for the other cases (not shown) are very similar (see Table 4).

Table 5). The ranges are 1362–1511 cm^{-1}, 1245–1302 cm^{-1} and 790–823 cm^{-1}, respectively. These values can be compared with the bands experimentally observed upon NO_2 adsorption on dispersed BaO catalysts centered at 1327, 1225 and 811 [1]. The charge of NO_2 present values around −0.95*e*, indicating that it adsorbs as nitrite anion (Table 5).

The high reactivity of peroxo groups present on the BaO particles is in agreement with experiments performed on defect-rich BaO, in which the surface peroxo group is observed to play an important role as center which activates NO to form NO_2 [2,4]. Furthermore, in other studies Yanagisawa observed an oxygen exchange of NO with surface oxygen in thermally activated powders of alkaline-earth oxides [45,46]. By using temperature-programmed desorption analysis he found an oxygen exchange of $N^{18}O$ with $Mg^{16}O$, $Ca^{16}O$ and $Sr^{16}O$. Although the mechanisms of this process have not been fully understood yet, it has been suggested that the exchange reactions proceed via NO_2 and NO_3 intermediates. Taking into account that a large amount of energy is

Table 5
Charges (q), and stretching (ν) and bending (δ) vibrational modes corresponding to the final state (adsorbed NO_2).

	Ba_6O_6(slab) edge		Ba_6O_6(slab) corner		BaO(hex)	
	O_a	O_s	O_a	O_s	O_a	O_s
q(N)	0.31	0.31	0.31	0.18	0.31	0.31
q(O)	−0.64	−0.64	−0.64	−0.44	−0.58	−0.70
$q(O_a)$	−0.64	−1.88	−0.64	−1.37	−0.68	−1.46
$q(O_s)$	−1.88	−0.64	−1.17	−0.70	−1.01	−0.57
$q(NO_2)$	−0.97	−0.97	−0.97	−0.96	−0.95	−0.96
ν_{asym}(N–O) (cm^{-1})	1363	1363	1362	1511	1382	1400
ν_{sym}(N–O)	1302	1302	1317	1245	1283	1288
δ(ONO)	813	813	790	795	823	821

required to extract a surface oxygen from the BaO surface, even with coordinatively unsaturated oxygen [30], it is likely that the lattice oxygen may come from surface peroxo groups formed during the thermal treatment.

4. Conclusions

Calculations indicate that NO reacts very easily with peroxo groups on Ba_6O_6 particles with either oxygen atom to form NO_2 by surpassing an activation barrier of only 0.2 eV or less. It turned to be of particular interest that NO_2 formed via the extraction of O_s because an interchange is produced between both oxygen atoms of surface peroxo. The predicted high reactivity is in agreement with experiments performed on highly defective BaO wherein NO activation is observed to occur on surface peroxo groups. Besides, it is likely that our theoretical results, evidencing the facile extraction of oxygen from BaO particles, could provide some clue to the observed isotopic exchange between oxygen atoms of NO and surface oxygen of thermally activated alkaline-earth oxides.

We hope that the present findings might stimulates further theoretical investigation about the reactivity of molecules such as NO, NO_2 and CO_2 with peroxo groups present on larger particles or on extended stepped surfaces of alkaline-earth oxides .

Acknowledgments

The authors acknowledge the financial support of CONICET, ANPCYT and Universidad Nacional del Sur (UNS).

References

[1] C. Hess, J.H. Lunsford, Mechanism for NO_2 storage in barium oxide supported on magnesium oxide studied by in situ Raman spectroscopy, J. Phys. Chem. B 106 (2002) 6358–6360.
[2] G. Mestl, M.P. Rosynek, J.H. Lunsford, Decomposition of nitric oxide over barium oxide supported on magnesium oxide. II – In situ Raman characterization of phases present during the catalytic reaction, J. Phys. Chem. B 101 (1997) 9321–9328.
[3] G. Mestl, M.P. Rosynek, J.H. Lunsford, Decomposition of nitric oxide over barium oxide supported on magnesium oxide. IV – In situ Raman characterization of oxide phase transitions and peroxide species by ^{18}O-labelling, J. Phys. Chem. B 102 (1998) 154–161.
[4] S. Xie, G. Mestl, M.P. Rosynek, J.H. Lunsford, Decomposition of nitric oxide over barium oxide supported on magnesium oxide. I – Catalytic results and in situ raman spectroscopic evidence for a barium-nitro intermediate, J. Am. Chem. Soc. 119 (1997) 10186–10191.
[5] F. Prinetto, G. Ghiotti, I. Nova, L. Lietti, E. Tronconi, P. Forzatti, FT-IR and TPD investigation of the NO_x storage properties of BaO/Al_2O_3 and $Pt–BaO/Al_2O_3$ catalysis, J. Phys. Chem. B 105 (2001) 12732–12745.
[6] C. Sedlmair, K. Seshan, A. Jentys, J.A. Lercher, Elementary steps of NO_x adsorption and surface reaction on a commercial storage–reduction catalyst, J. Catal. 214 (2003) 308–316.
[7] J.H. Kwak, D. Mei, C.W. Yi, D.H. Kim, C.H.F. Peden, L.F. Allard, J. Szanyi, Understanding the nature of surface nitrates in BaO/Al_2O_3 NO_x storage materials: a combined experimental and theoretical study, J. Catal. 261 (2009) 17–22.
[8] L. Olsson, H. Persson, E. Fridell, M. Skoglundh, B. Andersson, A kinetic study of NO oxidation and NO_x storage on Pt/Al_2O_3 and $Pt/BaO/Al_2O_3$, J. Phys. Chem. B 105 (2001) 6895–6906.
[9] H. Mahzoul, J.F. Brilhac, P. Gilot, Experimental and mechanistic study of NO_x adsorption over NO_x trap catalyst, Appl. Catal. B 20 (1999) 47–55.
[10] A. Amberntsson, H. Persson, P. Engstrom, B. Kasemo, NO_x release from a noble metal/BaO catalyst: dependence on gas composition, Appl. Catal. B 31 (2001) 27–38.
[11] C.W. Yi, J. Szanyi, BaO/Al_2O_3/NiAl(1 1 0) model NO_x storage materials: the effect of BaO film thickness on the amorphous-to-crystalline $Ba(NO_3)_2$ phase transition, J. Phys. Chem. C 113 (2009) 716–723.
[12] A. Tsami, F. Grillo, M. Bowker, R.M. Nix, Model NSR catalysts: fabrication and reactivity of barium oxide layers on Cu (1 1 1), Surf. Sci. 600 (2006) 3403–3418.
[13] P.J. Schmitz, R.J. Baird, NO and NO_2 adsorption on barium oxide: model study of the trapping stage of NO_x conversion via lean NO_x traps, J. Phys. Chem. B 106 (2002) 4172–4180.
[14] P. Broqvist, H. Grönbeck, E. Fridell, I. Panas, Characterization of NO_x species adsorbed on BaO: experiment and theory, J. Phys. Chem. B 108 (2004) 3523–3530.
[15] H. Grönbeck, P. Broqvist, I. Panas, Fundamental aspects of NO_x adsorption on BaO, Surf. Sci. 600 (2006) 403–408.
[16] P. Broqvist, I. Panas, E. Fridell, H.J. Persson, NO_x storage on BaO(1 0 0) surface from first principles: a two channel scenario, Phys. Chem. B 106 (2002) 137–145.
[17] M.M. Branda, C. Di Valentin, G. Pacchioni, NO and NO_2 adsorption on terrace, step, and corner sites of the BaO surface from DFT calculations, J. Phys. Chem. B 108 (2004) 4752–4758.
[18] R.M. Ferullo, S.A. Fuente, M.M. Branda, N.J. Castellani, Theoretical study of N_2O_2 interaction with BaO(1 0 0) surface, J. Mol. Struct. (Theochem) 818 (2007) 57–64.
[19] E.J. Karlsen, L.G.M. Pettersson, N_2O decomposition over BaO: including effects of coverage, J. Phys. Chem. B 106 (2002) 5719–5721.
[20] W.F. Schneider, Quantitative difference in the adsorption chemistry of acidic (CO_2, SO_x) and amphiphilic (NO_x) species on the alkaline earth oxides, Phys. Chem. B 108 (2004) 273–282.
[21] E.J. Karlsen, M.A. Nygren, L.G.M. Pettersson, Comparative study on structures and energetics of NO_x, SO_x, and CO_x adsorption on alkaline-earth-metal oxides, Phys. Chem. B 107 (2003) 7795–7802.
[22] M. Tutuianu, O.R. Inderwildi, W.G. Bessler, J. Warnatz, Competitive adsorption of NO, NO_2, CO_2, and H_2O on BaO(1 1 0): a quantum chemical study, J. Phys. Chem. B 110 (2006) 17484–17492.
[23] P. Broqvist, I. Panas, H. Grönbeck, The nature of NO_x species on BaO(1 0 0): an ab initio molecular dynamics study, J. Phys. Chem. B 109 (2005) 15410–15416.
[24] L.N. Kantorovich, M.J. Gillan, Adsorption of atomic and molecular oxygen on the MgO(0 0 1) surface, Surf. Sci. 374 (1997) 373–386.
[25] G. Geneste, J. Morillo, F. Finocchi, Adsorption and diffusion of Mg, O, and O_2 on the MgO(0 0 1) flat surface, J. Chem. Phys. 122 (2005) 174707–174718.
[26] D. Strömberg, The bonding and migration of an O atom on a CaO (1 0 0) surface. A theoretical study, Surf. Sci. 275 (1992) 473–481.
[27] N.X. Lu, G. Fu, X. Xu, H.L. Wan, Mechanisms for O_2 dissociation over the BaO(1 0 0) surface, J. Chem. Phys. 128 (2008) 034702–034711.
[28] E.J. Karlsen, M.A. Nygren, L.G.M. Petterson, Theoretical study on the decomposition of N_2O over alkaline earth metal–oxides: MgO–BaO, J. Phys. Chem. A 106 (2002) 7868–7875.
[29] W.S. Abdel Halim, A.S. Shalabi, The stability of peroxide ion O_2^{-2} at (1 1 0), (2 1 0) and (0 0 1) surfaces of MgO, CaO and SrO, Periodic ab initio calculations, Solid State Commun. 124 (2002) 67–72.
[30] C. Di Valentin, R. Ferullo, R. Binda, G. Pacchioni, Oxygen vacancies and peroxo groups on regular and low-coordinated sites of MgO, CaO, SrO, and BaO surfaces, Surf. Sci. 600 (2006) 1147–1154.
[31] Y.X. Li, J.R. Schlup, K.J. Klabunde, Fourier transform infrared photoacoustic spectroscopy study of the adsorption of organophosphorus compounds on heat-treated magnesium oxide, Langmuir 7 (1991) 1394–1399.
[32] K.J. Klabunde, J. Stark, O. Koper, C. Mohs, D.G. Park, S. Decker, Y. Jiang, I. Lagadic, D. Zhang, Nanocrystals as stoichiometric reagents with unique surface chemistry, J. Phys. Chem. 100 (1996) 12142–12153.
[33] P. Broqvist, H. Grönbeck, E. Fridell, I. Panas, NO_x storage on BaO: theory and experiment, Catal. Today 96 (2004) 71–78.
[34] R. Kakkar, P.N. Kapoor, K.J. Klabunde, First principle density functional study of the adsorption and dissociation of carbonyl compounds on magnesium oxide nanosurfaces, J. Phys. Chem. B 110 (2006) 25941–25949.
[35] R. Kakkar, P.N. Kapoor, K.J. Klabunde, Theoretical study of the adsorption of formaldehyde on magnesium oxide nanostructures: sizes effects and the role of low-coordinated and defect sites, J. Phys. Chem. B 108 (2004) 18140–18148.
[36] A.D. Becke, A new mixing of Hartree–Fock and local density-functional theories, J. Chem. Phys. 98 (1993) 1372–1378.
[37] M.J. Frisch et al., Gaussian 03, Revision C.02, Gaussian Inc., Wallingford, CT, 2004.
[38] F. Bawa, I. Panas, Competing pathways for MgO, CaO, SrO, and BaO nanocluster growth, Phys. Chem. Chem. Phys. 4 (2002) 103–108.
[39] P.J. Hay, W.R.J. Wadt, Ab initio effective core potentials for molecular calculations. Potentials for the transition metal atoms Sc to Hg, Chem. Phys. 82 (1985) 270–284.
[40] S.F. Boys, F. Bernardi, The calculation of small molecular interactions by the differences of separate total energies. Some procedures with reduced errors, Mol. Phys. 19 (1970) 553–566.

[41] S. Simon, M. Duran, J.J. Dannenberg, How does basis set superposition error change the potential surfaces for hydrogen-bonded dimers, J. Chem. Phys. 105 (1996) 11024–11031.
[42] A.E. Reed, L.A. Curtiss, F. Weinhold, Intermolecular interactions from a natural bond orbital, donor–acceptor view-point, Chem. Rev. 88 (1988) 899–926.
[43] C. Peng, P.Y. Ayala, H.B. Schlegel, M.J. Frisch, Using redundant internal coordinates to optimize equilibrium geometries and transition states, J. Comp. Chem. 17 (1996) 49–56.
[44] M. Nakamura, H. Mitsuhashi, N. Takezawa, Oxygen species formed on different surface sites of CaO by decomposition of N_2O, J. Catal. 138 (1992) 686–693.
[45] Y. Yanagisawa, NO interaction with thermally activated CaO and SrO surfaces, Appl. Surf. Sci. 100 (101) (1996) 256–259.
[46] Y. Yanagisawa, Oxygen exchange between adsorbed NO and MgO surfaces, Appl. Surf. Sci. 89 (1995) 251–253.